JOURNAL OF VIROLOGY, July 2011, p. 7162–7168 Vol. 85, No. 14
0022-538X/11/$12.00 doi:10.1128/JVI.00051-11

Canine Distemper Virus Matrix Protein Influences Particle Infectivity, Particle Composition, and Envelope Distribution in Polarized Epithelial Cells and Modulates Virulence▽

Erik Dietzel,[1]‡ Danielle E. Anderson,[2]‡† Alexandre Castan,[2] Veronika von Messling,[2]†* and Andrea Maisner[1]*

Institute of Virology, Philipps University Marburg, Marburg, Germany,[1] and INRS-Institut Armand-Frappier, University of Quebec, Laval, Quebec, Canada[2]

Received 10 January 2011/Accepted 22 April 2011

In paramyxoviruses, the matrix (M) protein mediates the interaction between the envelope and internal proteins during particle assembly and egress. In measles virus (MeV), M mutations, such as those found in subacute sclerosing panencephalitis (SSPE) strains, and differences in vaccine and wild-type M proteins can affect the strength of interaction with the envelope glycoproteins, assembly efficiency, and spread. However, the contribution of the M protein to the replication and pathogenesis of the closely related canine distemper virus (CDV) has not been characterized. To this end this, we generated a recombinant wild-type CDV carrying a vaccine strain M protein. The recombinant virus retained the parental growth phenotype in VerodogSLAMtag cells, but displayed an increased particle-to-infectivity ratio very similar to that of the vaccine strain, likely due to inefficient H protein incorporation. Even though infectious virus was released only from the apical surface, consistent with the release polarity of the wild-type CDV strain, envelope protein distribution in polarized epithelial cells reproduced the bipolar pattern seen in vaccine strain-infected cells. Most notably, the chimeric virus was completely attenuated in ferrets and caused only a mild and transient leukopenia, indicating that the differences in particle infectivity and envelope protein sorting mediated by the vaccine M protein contribute importantly to vaccine strain attenuation.

Morbilliviruses are enveloped negative-strand RNA viruses that cause severe disease in their respective hosts. Pathogenesis studies of measles virus (MeV) in nonhuman primates and canine distemper virus (CDV) in ferrets reveal that wild-type strains initially target immune cells and then spread to epithelia and in some cases to the central nervous system (6, 23, 34). This dissemination requires the transition of the respiratory mucosa at the initial infection stage, subsequent spread to lymphoid and epithelial tissues throughout the body, and finally virus release via the epithelia of the respiratory, gastrointestinal, and urinary tracts for shedding and transmission.

Polarized epithelia form barriers that separate compartments within the organism, as well as the organism and the environment (22). Consequently, replication in epithelia constitutes an integral part of the life cycle of many viruses. The polarization of the epithelial layer results in distinct apical and basolateral domains that are separated by tight junctions, and membrane proteins are transported to the apical or basolateral surface based on sorting signals in their sequences (14). Many viruses exploit this polarization by recognizing receptor molecules that are localized at the respective site of contact with the epithelial layer (7, 11, 32). It is further speculated that virus dissemination either by lateral cell-to-cell fusion or by polarized virus release from epithelia contributes to virulence (5, 9, 13, 30).

The matrix (M) protein plays an essential role in paramyxovirus assembly by mediating the interaction of the viral ribonucleoprotein complex with plasma membrane regions containing the viral glycoproteins (10). For MeV, it has been shown that mutations in the M protein, such as those identified in subacute sclerosing panencephalitis (SSPE) strains, or deletion of the entire protein disrupt virus assembly and influence pathogenicity (3, 18, 20). In polarized epithelial cells, the localization of M rather than the innate sorting signals in the viral glycoproteins determines their membrane distribution and budding polarity (12, 16, 19). In addition, MeV wild-type and vaccine M proteins interact differently with the viral glycoproteins, thereby influencing virus spread and particle assembly in cell culture (28).

In contrast to MeV, the role of the M protein in vaccine and wild-type CDV strains has not been investigated. To characterize the contributions of the different M protein functions to pathogenesis, we generated a recombinant wild-type CDV carrying the M protein of the vaccine strain Onderstepoort (OS). We first compared growth characteristics and particle compositions *in vitro* and assessed the release polarity and envelope protein distribution in polarized epithelial cells. The pathogenesis of the parental and recombinant viruses was then evaluated in ferrets.

* Corresponding author. Mailing address for V.V.M.: INRS-Institut Armand-Frappier, University of Quebec, 531, boul. des Prairies, Laval, Quebec H7V 1B7, Canada. Phone: (450) 687-5010. Fax: (450) 686-5309. E-mail: veronika.vonmessling@iaf.inrs.ca. Mailing address for A.M.: Institute of Virology, Philipps University Marburg, Hans-Meerwein-Str. 2, D-35043 Marburg, Germany. Phone: 49-6421-2865360. Fax: 49-6421-2868962. E-mail: maisner@staff.uni-marburg.de.

‡ E.D. and D.E.A. contributed equally to this work.

† Present address: Emerging Infectious Disease Program, Duke-NUS Graduate Medical School, Singapore.

▽ Published ahead of print on 4 May 2011.

MATERIALS AND METHODS

Cells and viruses. VerodogSLAMtag cells (36) and 293 cells (ATCC CRL-1573) were maintained in Dulbecco's modified Eagle's medium (DMEM) (Invitrogen) with 5% fetal calf serum (FCS) (Invitrogen). Madin-Darby canine kidney (MDCK II) cells were grown in Eagle's minimal essential medium (MEM) (Gibco) containing 10% fetal calf serum (FCS), 100 units penicillin ml^{-1}, and 0.1 mg streptomycin ml^{-1}. For polarized cultures, cells were seeded on 1-μm-pore-size filter supports (ThinCerts Tissue Culture Inserts; Greiner Bio-One). The parental recombinant viruses, 5804PeH (34) and OS (38), and all recombinant mutants constructed in this study were propagated in VerodogSLAMtag cells.

Generation of recombinant viruses. The CDV 5804PeH plasmid (34) constituted the basis for the construction of the chimeric virus. Overlap extension PCR (8) was used to produce the recombinant 5804/OS PCR fragments, which were then introduced into the SpeI and SalI restriction sites of the 5804PeH genome. The recombinant virus, composed of the 5804PeH backbone and the OS M open reading frame (ORF), was named 58MOS. The recombinant 58MOS virus was recovered as previously outlined (1). Briefly, semiconfluent 293 cells in 6-well plates were transfected with 4 μg of recombinant full-length CDV genome plasmid in combination with 0.5, 0.1, 0.5, and 0.7 μg, respectively, of MeV N, P, polymerase (L), and T7 polymerase expression plasmids, using Lipofectamine 2000 (Invitrogen). Two days posttransfection, the cells were trypsinized and seeded onto 100-cm^2 plates, together with 5×10^6 VerodogSLAMtag cells. The cocultures were maintained in DMEM containing 5% FCS until syncytia were observed. The syncytia were then transferred onto fresh VerodogSLAMtag cells to produce virus stocks.

For virus kinetics, VerodogSLAMtag cells were infected at a multiplicity of infection (MOI) of 0.01 50% tissue culture infective dose ($TCID_{50}$), samples were harvested daily for 5 days following the infection, and the cell-associated and cell-free titers were determined by limited dilution. Photographs were taken using an Eclipse TE2000-U compound microscope with a DXM1200F digital camera (Nikon).

Virus purification. VerodogSLAMtag cells in 100-cm^2 plates were infected with the different viruses at an MOI of 0.01 $TCID_{50}$. Supernatant was harvested when the cytopathic effect (CPE) reached 80% and clarified by centrifugation at $2{,}000 \times g$ for 30 min at 4°C. The supernatant was loaded onto a 20% (wt/vol) sucrose cushion and centrifuged at $134{,}000 \times g$ for 2 h at 4°C. The purified virus pellet was resuspended in 100 μl phosphate-buffered saline (PBS) (Invitrogen), the viral titer was determined by the limited-dilution method and expressed as $TCID_{50}$, and the protein concentration was quantified using the bicinchoninic acid (BCA) assay (Pierce).

Polyacrylamide gel electrophoresis and Western blotting. Proteins from purified virions were separated by 10% SDS-polyacrylamide gel electrophoresis and transferred to an Immobilon-P polyvinylidene difluoride (PVDF) membrane (Millipore Corporation). The membranes were blocked with 5% skim milk in TBS-T (50 mM Tris-HCl, pH 7.4, 150 mM NaCl, 0.1% Tween 20) and incubated with CDV nucleoprotein (N)-, fusion (F) protein-, or hemagglutinin (H) protein-specific rabbit anti-peptide serum (1) or with an M protein-specific mouse monoclonal antibody (MAB8910; Millipore), followed by horseradish peroxidase-conjugated secondary antibodies. The proteins were visualized using the ECL Plus Western Blotting Detection system (GE Healthcare), exposed on a luminescent-image analyzer (Kodak), and quantified using Molecular Imaging software (Kodak).

Electron microscopic analysis. For electron microscopic (EM) analysis, viruses were purified as described above. Virus pellets were resuspended in PBS, fixed with 4% paraformaldehyde for 15 min, and deposited on Formvar-coated nickel grids for 10 min. The excess fluid was blotted away with Whatman filter paper, and the grids were incubated for 5 min with 0.1 M glycine in PBS to quench aldehyde groups, followed by an overnight incubation in blocking buffer (2% bovine serum albumin, 0.2% Tween 20, 5% glycerol, and 0.05% sodium azide in PBS). After being washed with PBS, samples were negatively stained with 2% phosphotungstic acid solution and examined with a Zeiss 109 electron microscope.

Immunofluorescence analysis of polarized MDCK cells. MDCK cells were infected and seeded onto ThinCerts filter supports. To monitor cell polarization, the transepithelial resistance (TER) was controlled daily using a Millipore-ERS apparatus (Millipore). Analyses at day 6 after seeding were performed only with cells that gave TER values above 180 $\Omega \cdot cm^2$. To detect cell-to-cell fusion in epithelia, CDV-infected MDCK cells were fixed with 2% paraformaldehyde and then incubated from both sides with a rabbit antiserum against CDV-H (38). The primary antibodies were detected with Alexa-Fluor 568-coupled secondary antibodies (Invitrogen). To visualize cell junctions, cells were incubated with a monoclonal antibody against E-cadherin (BD Biosciences Pharmingen). Bound primary antibodies were detected with an Alexa-Fluor 488-conjugated goat antiserum directed against mouse IgG (Invitrogen). The filters were cut out from their supports, mounted onto microscope slides in Mowiol 4-88 (Calbiochem), and analyzed using a Zeiss Axiovert 200M microscope.

To analyze envelope protein distribution in infected polarized MDCK cells, the H and F proteins were detected using a rabbit anti-peptide serum or a mouse monoclonal antibody, respectively, recognizing peptides in the extracellular domain of the respective proteins (33, 38), while the M protein was marked with the M protein-specific monoclonal antibody (MAB8910; Millipore) after fixation of the cells with 2% paraformaldehyde and subsequent permeabilization with 0.2% Triton X-100. Bound primary antibodies were detected with appropriate Alexa-Fluor 568-labeled secondary antibodies and analyzed with a confocal laser scanning microscope (LSM510Meta; Zeiss).

Animal experiments and assessment of virulence. Unvaccinated ferrets (*Mustela putorius furo*) 16 weeks old and older (Marshall Farms) were used for all studies. The experiments were performed as described previously (36) and were approved by the Institutional Animal Care and Use Committee of the INRS-Institut Armand-Frappier. Groups of three or four animals were infected intranasally with 10^5 $TCID_{50}$ of each virus. Body temperature and clinical signs were recorded daily, and blood samples were collected from the jugular vein under general anesthesia twice weekly for the first 2 weeks postinfection and weekly thereafter. Besides body temperature, three parameters of virulence were measured and graded. Rash was graded as 0 (no rash), 1 (localized rash), or 2 (generalized rash). Weight loss was classified as 0 (0 to 5% loss of day 0 body weight), 1 (5 to 10% loss of day 0 body weight), or 2 (more than 10% loss of day 0 body weight). Cell-associated viremia was determined by limiting dilution of peripheral blood mononuclear cells (PBMCs) as previously described (37).

RESULTS

The vaccine M protein does not affect the wild-type syncytium phenotype and growth characteristics but changes the particle-to-infectivity ratio and particle composition. CDV M proteins display only 3% amino acid variability, and the OS vaccine and 5804P wild-type strains differ at six positions (Fig. 1A), none of which is close to a putative late domain (amino acids [aa] 20 to 23, 23 to 26, 52 to 55, 311 to 314, and 332 to 335 [25]); to other functional motifs identified in closely related M proteins (V_{101}VRT [24]); or to residues 64 and 89, which differ between MeV vaccine and wild-type strains (28). To assess the contribution of M to the polarity of CDV epithelial cell release and pathogenesis, a recombinant virus carrying the OS M protein in the 5804P background was generated (Fig. 1B). In VerodogSLAMtag cells, the chimeric and parental viruses displayed similar syncytial phenotypes and growth kinetics of cell-associated and released virus (Fig. 1C and D), indicating that the chimeric virus retained the parental growth phenotype.

Since paramyxovirus M proteins play an important role in particle formation (10), the particle-to-infectivity ratios of the parental and chimeric viruses were evaluated. To this end, virus particles produced in VerodogSLAMtag cells were purified by sucrose gradient ultracentrifugation, and 100 $TCID_{50}$ of each virus was loaded on an SDS-PAGE gel and subjected to Western blot analysis using a CDV N protein-specific rabbit antiserum. OS and 58MOS samples contained around 10 times more N protein than 5804P samples (Fig. 2A), indicating that the presence of the OS M results in an increase in the formation of noninfectious particles. To determine if this decreased particle-to-infectivity ratio is due to differences in the M incorporation into viral particles, the protein composition of purified virions was analyzed by using equal protein quantities for Western blot analysis. While the relative M/N and F/N ratios were similar between 5804P and 58MOS, OS particles contained five times more M and only half the amount of F protein

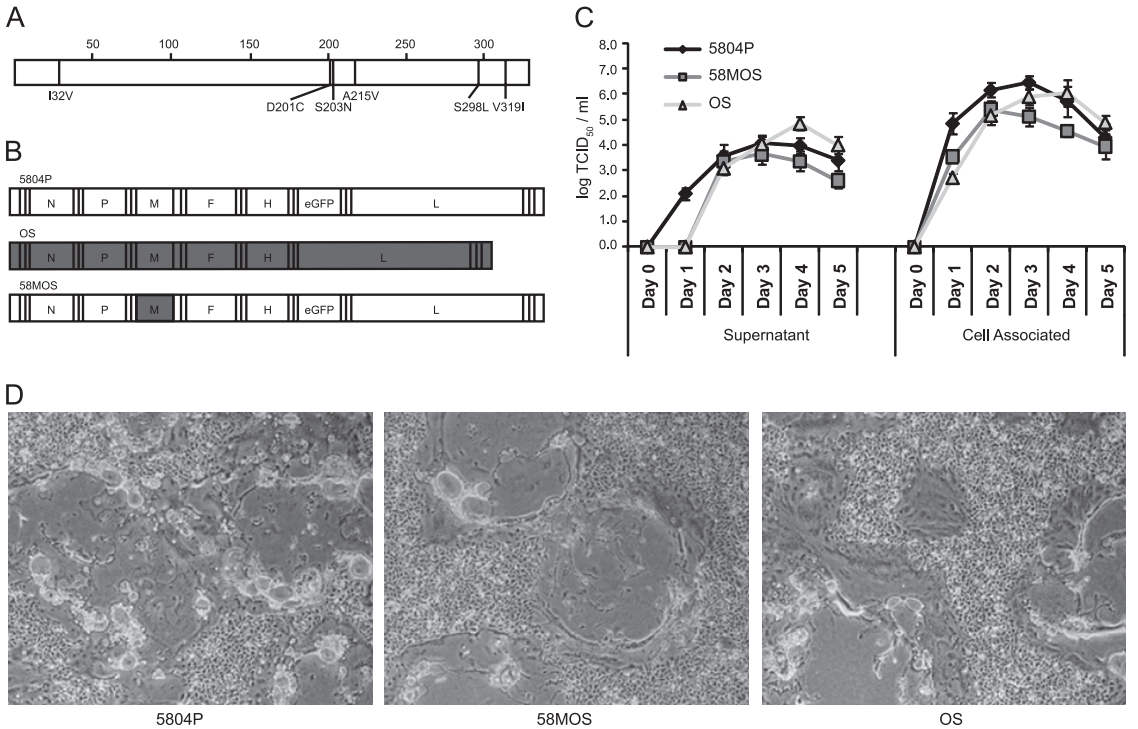

FIG. 1. Characterization of the chimeric virus. (A) Localization of the M protein amino acid differences between OS and 5804P. The position of each divergent amino acid is indicated as a line in the M protein cartoon, and the OS amino acid is shown underneath, followed by the exact position and the corresponding 5804P amino acid. (B) Schemes of the parental and recombinant viruses used in this study. The white boxes indicate 5804P genetic origin, gray boxes OS genetic origin. (C and D) Syncytium phenotype and growth kinetics of the parental and recombinant viruses. VerodogSLAMtag cells were infected at an MOI of 0.01. (C) Cell-associated and released virus kinetics. Samples were harvested daily for 5 days after infection, and virus titers were determined by the $TCID_{50}$ method. The error bars indicate standard deviations. (D) Extent of syncytium formation 3 days after infection (magnification, ×40).

(Fig. 2B). However, compared to 5804P, 58MOS and OS particles contained much smaller amounts of H protein, yielding H/N ratios of 0.05 and 0.27, respectively. A comparison of purified virus particles by electron microscopy after negative staining yielded no obvious differences in virion morphology (Fig. 2C) or presence of virus-like particles lacking RNPs (data not shown). However, a slight increase in free viral nucleocapsids was observed in the 58MOS preparations (Fig. 2C, inset), suggesting that 58MOS particles are more fragile. Taken together, these analyses indicate that the OS M protein is less efficient in interacting with H, thus resulting in decreased H protein incorporation, which in turn, either *per se* or due to a markedly altered H/F ratio, leads to decreased particle infectivity.

The polarity of virus release differs between wild-type and vaccine strains. Since MeV predominantly buds from the apical surfaces of polarized epithelial cells (2, 12, 16, 29), the release polarities of the parental and chimeric CDV strains were characterized in polarized MDCK cells, which are natural host cells for CDV and a well-established model for epithelial polarity (21). MDCK cells infected with 5804P, 58MOS, and OS were able to establish a polarized monolayer, as determined by transepithelial resistance above 180 $\Omega \cdot cm^2$. To visualize cell-to-cell fusion in epithelia, we performed a double staining with an antibody against the adherens junction molecule E-cadherin and an antiserum against CDV-H 6 days after seeding. At this time point, multiple infected foci with little or no syncytium formation were detectable for each virus, while the tight junctions were still intact, as illustrated by the characteristic honeycomb pattern (Fig. 3A). To determine the extent of virus release from the apical or basolateral cell surface, infected cells were grown for 4 days until the cell monolayer was fully polarized. The culture medium was then replaced, and the cell-free virus produced between 96 h and 120 h and 120 h and 144 h postseeding was quantified by plaque titration. While all three viruses were detected in apical cell supernatants with titers ranging between 4×10^4 and 1×10^5 PFU, only OS was also released in the basal filter chamber, albeit at a 17-fold-reduced titer (Fig. 3B). This clearly shows that introduction of the OS M protein into wild-type CDV does not alter cell-to-cell spread or budding polarity in polarized MDCK cells.

The M protein determines envelope protein surface distribution in polarized epithelial cells. While sorting signals in the cytoplasmic tails of the viral glycoproteins determine their localization in polarized epithelial cells when expressed individually, the intracellular M protein distribution correlates with release orientation in MeV-infected polarized cells (16, 19). To assess whether the bipolar release of OS is due to differences in CDV envelope protein distribution, the membrane localization of the H, F, and M proteins was analyzed in polarized MDCK cells infected with the respective viruses. To this end, samples were fixed 6 days after being seeded on filter supports; stained from both sides

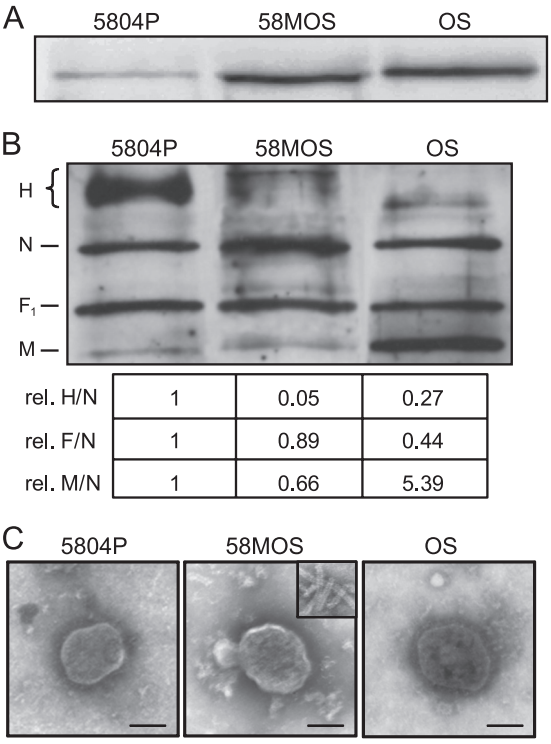

rel. H/N	1	0.05	0.27
rel. F/N	1	0.89	0.44
rel. M/N	1	0.66	5.39

FIG. 2. Protein compositions and EM analyses of purified virions. (A and B) Western blot analyses of purified virus particles. Released virus was purified through a 20% sucrose cushion. For particle-to-infectivity ratio determination (A) and comparison of the viral protein ratios (B), 100 $TCID_{50}$ or equal protein amounts, respectively, of each sample were separated by SDS-PAGE, and N, F_1, H, and M proteins were detected by Western blot analysis using protein-specific antisera. Viral proteins were visualized by enhanced chemiluminescence (ECL), and protein bands were densitometrically quantified. The relative (rel.) optical densities of the H, F, and M bands per optical density of the corresponding N bands are shown below, with the ratios of the wild type set as 1. (C) EM analysis of purified virus particles. Samples on Formvar-coated nickel grids were contrasted using phosphotungstic acid. The inset shows free viral nucleocapsids found only in the 58MOS preparations. Bar, 100 nm.

with antibodies against the M, H, and F proteins, respectively; and analyzed by confocal microscopy. Western blot analysis of samples harvested at the same time revealed similar amounts of M, F, and H proteins for all viruses (data not shown). Consistent with the strictly apical virus release observed for 5804P, the confocal vertical sections (side views) clearly demonstrate that all three 5804P envelope proteins are exclusively expressed at the apical cell surface (Fig. 4, left). In contrast, and consistent with its bipolar release pattern, all OS envelope proteins were found on apical and basolateral membranes (Fig. 4, right). This bipolar M protein distribution pattern was also observed for 58MOS, indicating that the targeting information resides in the M protein itself (Fig. 4, middle). Thus, the presence of the OS M protein alone is sufficient to retarget the wild-type F and, to a lesser extent, H proteins to the basolateral membranes, demonstrating its central role in assembly.

The M protein contributes importantly to virulence. To assess the impacts of the observed differences in particle-to-infectivity ratios and envelope protein distributions on pathogenesis, groups of three or four ferrets were inoculated intranasally with 10^5 $TCID_{50}$ of the respective viruses. As reported previously (38), the body temperatures of animals infected with 5804P increased steadily up to 40.5°C (Fig. 5B). The animals also developed severe signs of disease, including weight loss of more than 15% and generalized rash, reaching experimental endpoints for euthanasia between 12 and 16 days after infection (Fig. 5A). In total contrast, neither OS nor 58MOS resulted in detectable signs of clinical disease, other than a transient phase of slightly increased temperature around day 8 after infection (Fig. 5A and B). All viruses resulted in a drop in leukocyte counts within the first week after infection, but the values stabilized or even recovered during the subsequent week in OS- and 58MOS-infected animals while remaining low in the 5804P group (Fig. 5C). Both parental viruses resulted in sustained cell-associated viremia in PBMCs, with 5804P-infected animals reaching titers of over 10^5 $TCID_{50}$ per 10^6 PBMCs (Fig. 5D). Even though the OS-associated titers were 100-fold reduced, the animals were viremic for more than 7 days. In contrast, virus was detected in the PBMCs of only one 58MOS-infected animal, suggesting, especially taking into account the mild and short-lived leukopenia, that the chimeric virus is even more attenuated than the parental vaccine strain.

DISCUSSION

The importance of matrix proteins for particle assembly and egress of enveloped viruses is increasingly recognized, but little is known about its contribution to pathogenesis. Here, we show that replacement of the endogenous M protein with a vaccine strain M protein in a wild-type CDV not only increases the particle-to-infectivity ratio, likely due to decreased H protein incorporation, and leads to vaccine-like envelope glycoprotein distribution in polarized cells, but also results in complete attenuation in ferrets.

Two mutations found in the M proteins of MeV vaccine strains resulted in a stronger interaction with the H protein, thereby specifically increasing virus production (28). In CDV, there are 6 amino acid differences between the M proteins of vaccine and wild-type strains. None of them is close to those found in MeV, and the increased particle-to-infectivity ratio, the reduced glycoprotein particle content, and the basolateral sorting of envelope glycoproteins observed in our study indicate that the differences in the CDV vaccine M protein result in a less efficient interaction with the viral glycoproteins. In this respect, the CDV vaccine strain is similar to SSPE-inducing MeV strains, where changes in the M and F genes result in almost complete loss of infectious MeV particle production (4). A recombinant MeV lacking the M protein also reproduced this phenotype (3), demonstrating the key role of the M protein in particle assembly. A comparative analysis in monocyte-derived dendritic cells revealed a lack of virus production in MeV vaccine strain-infected cells, while infection with wild-type strains resulted in sustained virus production, despite similar initial infection levels (17). There is thus mounting evidence that high levels of viral protein production due to rapid cell-to-cell spread combined with an increased release of noninfectious particles contributes to the high immunogenicity of the *Morbillivirus* vaccine strains and, consequently, to their attenuation.

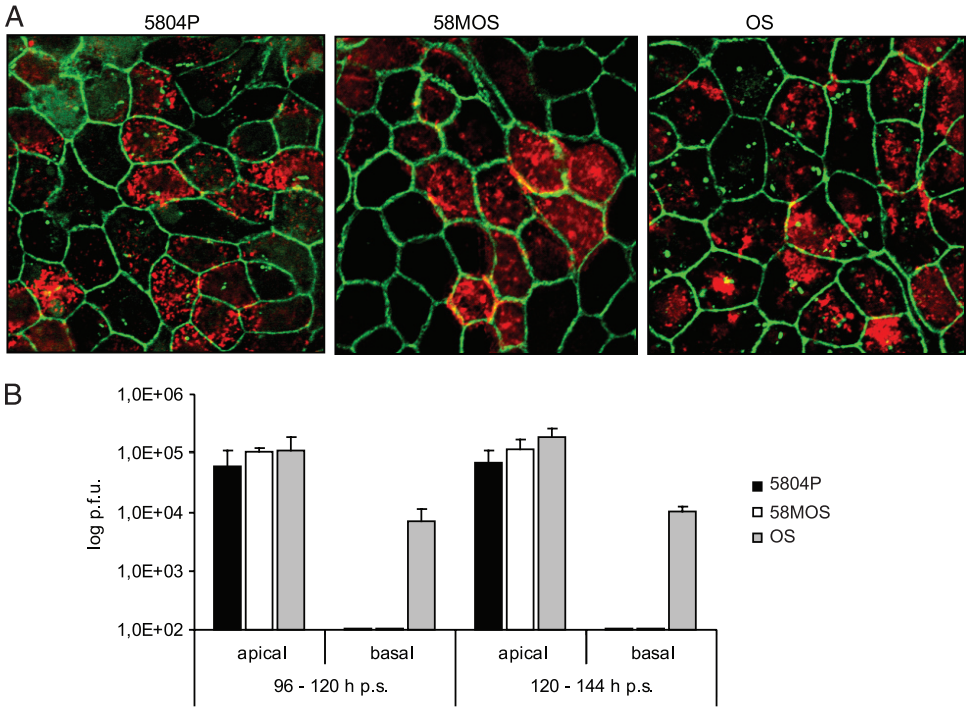

FIG. 3. CDV spread and release in polarized MDCK cells. (A) MDCK cells were infected with 5804P, 58MOS, or OS and cultivated on permeable filter supports for 6 days. The cells were then paraformaldehyde fixed, and infected cells were detected with a rabbit antiserum against CDV-H, followed by an Alexa-Fluor 568-coupled secondary antibody. Cell junctions were visualized with a mouse antibody against E-cadherin and an Alexa-Fluor 488-labeled secondary antibody. A composite image of CDV-positive cells and cell junction staining at ×630 magnification is shown. (B) Quantification of virus release from apical and basolateral membrane surfaces. Released virus was quantified by plaque assay on days 5 (96 to 120 h) and 6 (120 to 144 h) postseeding (p.s.). The results represent the average of three experiments, and the error bars indicate the standard deviations.

In *Morbillivirus* pathogenesis, spread from the initially targeted signaling lymphocytic activation molecule (CD150) (SLAM)-expressing immune cells (31) to epithelial tissues coincides with the onset of clinical signs (6, 36), and lack of epithelial cell infection abolishes shedding (11). CDV is an attractive model system to investigate the importance of interactions between morbilliviruses and polarized epithelia for virulence and attenuation in more detail, since MDCK cells originate from dogs, one of its natural hosts, and support replication of vaccine and wild-type strains. In polarized MDCK cells, the wild-type CDV strain was released only from the apical side, consistent with reports of MeV release patterns (11, 12, 27), while the OS vaccine strain was also detected in the basolateral compartment, albeit at a 17-fold-lower titer. Consistent with this observation, the OS M protein is expressed apically and basolaterally, whereas the wild-type M protein is present only at apical surfaces of polarized cells. This importance of the M protein for the polarity of particle release has been demonstrated for a variety of viruses (15, 16, 26, 40).

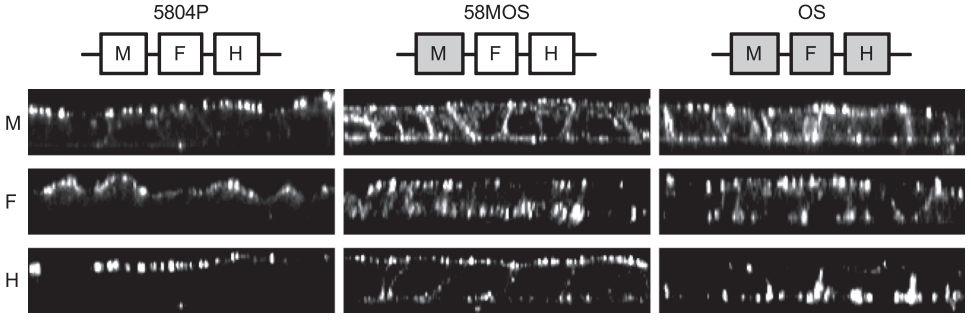

FIG. 4. Distribution of CDV envelope proteins in polarized MDCK cells. 5804P-, 58MOS-, or OS-infected MDCK cells were cultivated on permeable filter supports for 6 days. The cells were then stained with a mouse monoclonal antibody or a rabbit anti-peptide serum against the CDV F or H protein, respectively, or after paraformaldehyde fixation and permeabilization with a monoclonal antibody against the M protein, followed by staining with appropriate Alexa-Fluor 568-coupled secondary antibodies. The images show vertical sections through the cell monolayer (side views, *xz* scans) produced by a Zeiss LSM510 confocal laser scanning microscope (magnification, ×630). The envelope composition of each virus is indicated above the images.

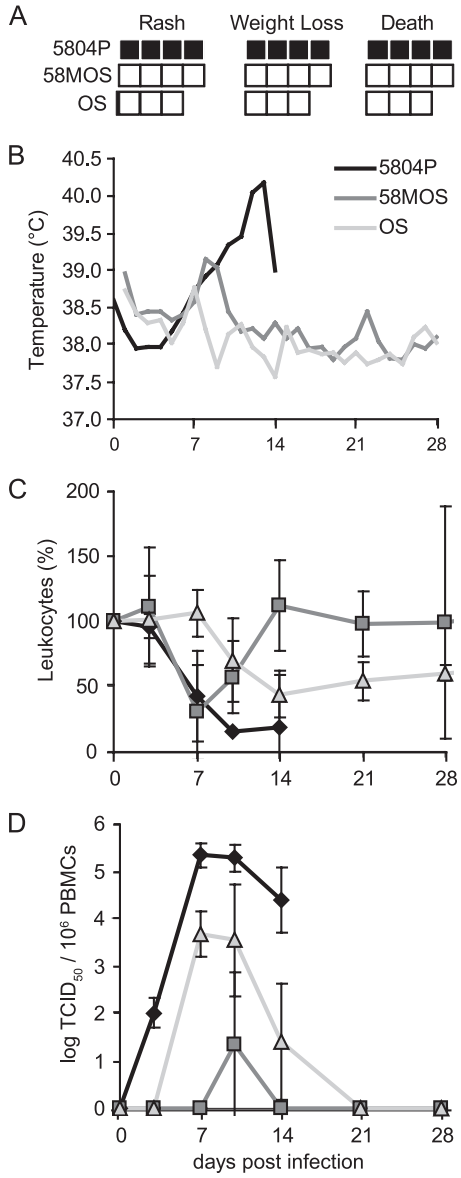

FIG. 5. Virulence and course of disease in ferrets. Groups of three or four animals were infected intranasally with 10^5 $TCID_{50}$ of either 5804P, 58MOS, or OS. (A) Virulence index. Each box represents one animal, and black represents the highest (2), gray an intermediate (1), and white the lowest (0) score for the respective criteria, as detailed in Materials and Methods. (B) Rectal temperatures were recorded daily. (C) Leukopenia in animals infected with the different viruses. Leukocyte counts at day 0 postinfection (p.i.) were set as 100% for each animal. (D) The course of cell-associated viremia is shown as the $\log_{10}$ of the virus titer per 10^6 PBMCs. The error bars indicate the standard deviations.

However, despite bipolar OS M protein expression, the chimeric 58MOS was still released only apically, indicating that M localization alone is not sufficient for release of infectious particles from the basolateral surface. In fact, basolateral release of infectious virus also requires substantial basolateral expression of both viral glycoproteins, which is found only in OS-infected cells. We have recently shown for Nipah virus that paramyxovirus glycoprotein redistribution in polarized cells can be induced by syncytium formation (39), but the lack of syncytium formation in CDV-infected polarized MDCK cells prevents the resulting loss of cell polarity and subsequent changes in viral glycoprotein distribution. Instead, retargeting is likely triggered by direct interactions of the M protein with the viral glycoproteins, as has been proposed for several viral matrix proteins (9, 16, 39). The less efficient retargeting of the wild-type H protein observed in our study is consistent with the particle composition analysis, indicating that the vaccine M protein is impaired in its ability to interact with H and is the most likely reason for the lack of basolateral release of infectious virus in 58MOS-infected cells. Thus, M protein-mediated alteration of viral glycoprotein distribution may contribute to vaccine strain attenuation, even though the particle release polarity remains unchanged.

Introduction of the vaccine M protein into a lethal wild-type strain resulted in complete attenuation. In fact, the chimeric virus resulted in lower cell-associated viremia and less leukopenia than the vaccine strain, illustrating not only the overall contribution of M to virulence, but also the importance of the coevolution of viral proteins. The increased production of noninfectious particles, in combination with the bipolar expression of M and F, and to a lesser extent also the H proteins observed for 58MOS *in vitro*, leads us to suggest the following model for 58MOS attenuation. Increased production of noninfectious virus particles, accompanied by additional basolateral expression of viral surface glycoproteins in epithelial cells, facilitates immune recognition by exposing increased amounts of viral antigens to immune cells, thereby supporting faster virus clearance.

ACKNOWLEDGMENTS

We are grateful to Larissa Kolesnikova for her help with the EM analysis.

This work was supported by grants from the German Research Foundation (DFG) to A.M. (MA 1886/6-1) and by grants to V.V.M. from the Canadian Institutes of Health Research (MOP-66989) and the Canadian Foundation for Innovation (9488).

REFERENCES

1. **Anderson, D. E., and V. von Messling.** 2008. Region between the canine distemper virus M and F genes modulates virulence by controlling fusion protein expression. J. Virol. **82:**10510–10518.
2. **Blau, D. M., and R. W. Compans.** 1995. Entry and release of measles virus are polarized in epithelial cells. Virology **210:**91–99.
3. **Cathomen, T., et al.** 1998. A matrix-less measles virus is infectious and elicits extensive cell fusion: consequences for propagation in the brain. EMBO J. **17:**3899–3908.
4. **Cathomen, T., H. Y. Naim, and R. Cattaneo.** 1998. Measles viruses with altered envelope protein cytoplasmic tails gain cell fusion competence. J. Virol. **72:**1224–1234.
5. **Chan, M. C., et al.** 2009. Influenza H5N1 virus infection of polarized human alveolar epithelial cells and lung microvascular endothelial cells. Respir. Res. **10:**102.
6. **de Swart, R. L., et al.** 2007. Predominant infection of CD150+ lymphocytes and dendritic cells during measles virus infection of macaques. PLoS Pathog. **3:**e178.
7. **Excoffon, K. J., et al.** 2008. Reovirus preferentially infects the basolateral surface and is released from the apical surface of polarized human respiratory epithelial cells. J. Infect. Dis. **197:**1189–1197.
8. **Horton, R. M., H. D. Hunt, S. N. Ho, J. K. Pullen, and L. R. Pease.** 1989. Engineering hybrid genes without the use of restriction enzymes: gene splicing by overlap extension. Gene **77:**61–68.
9. **Kolesnikova, L., E. Ryabchikova, A. Shestopalov, and S. Becker.** 2007. Basolateral budding of Marburg virus: VP40 retargets viral glycoprotein GP to the basolateral surface. J. Infect. Dis. **196**(Suppl. 2):S232–S236.
10. **Lamb, R. A., and G. D. Parks.** 2007. *Paramyxoviridae*: the viruses and their replication, p. 1449–1496. *In* D. M. Knipe, P. M. Howley, D. E. Griffin, R. A. Lamb, M. A. Martin, B. Roizman, and S. E. Straus (ed.), Fields virology, 5th ed., vol. 1. Lippincott Williams & Wilkins, Philadelphia, PA.
11. **Leonard, V. H., et al.** 2008. Measles virus blind to its epithelial cell receptor remains virulent in rhesus monkeys but cannot cross the airway epithelium and is not shed. J. Clin. Invest. **118:**2448–2458.

12. **Maisner, A., H. Klenk, and G. Herrler.** 1998. Polarized budding of measles virus is not determined by viral surface glycoproteins. J. Virol. **72:**5276–5278.
13. **McGraw, H. M., and H. M. Friedman.** 2009. Herpes simplex virus type 1 glycoprotein E mediates retrograde spread from epithelial cells to neurites. J. Virol. **83:**4791–4799.
14. **Mellman, I., and W. J. Nelson.** 2008. Coordinated protein sorting, targeting and distribution in polarized cells. Nat. Rev. Mol. Cell Biol. **9:**833–845.
15. **Mora, R., E. Rodriguez-Boulan, P. Palese, and A. Garcia-Sastre.** 2002. Apical budding of a recombinant influenza A virus expressing a hemagglutinin protein with a basolateral localization signal. J. Virol. **76:**3544–3553.
16. **Naim, H. Y., E. Ehler, and M. A. Billeter.** 2000. Measles virus matrix protein specifies apical virus release and glycoprotein sorting in epithelial cells. EMBO J. **19:**3576–3585.
17. **Ohgimoto, K., et al.** 2007. Difference in production of infectious wild-type measles and vaccine viruses in monocyte-derived dendritic cells. Virus Res. **123:**1–8.
18. **Patterson, S., A. Rae, N. Hockey, J. Gilmour, and F. Gotch.** 2001. Plasmacytoid dendritic cells are highly susceptible to human immunodeficiency virus type 1 infection and release infectious virus. J. Virol. **75:**6710–6713.
19. **Riedl, P., M. Moll, H. D. Klenk, and A. Maisner.** 2002. Measles virus matrix protein is not cotransported with the viral glycoproteins but requires virus infection for efficient surface targeting. Virus Res. **83:**1–12.
20. **Rima, B. K., and W. Paul Duprex.** 2005. Molecular mechanisms of measles virus persistence. Virus Res. **111:**132–147.
21. **Rodriguez-Boulan, E., G. Kreitzer, and A. Musch.** 2005. Organization of vesicular trafficking in epithelia. Nat. Rev. Mol. Cell Biol. **6:**233–247.
22. **Rodriguez-Boulan, E., and W. J. Nelson.** 1989. Morphogenesis of the polarized epithelial cell phenotype. Science **245:**718–725.
23. **Rudd, P. A., R. Cattaneo, and V. von Messling.** 2006. Canine distemper virus uses both the anterograde and the hematogenous pathway for neuroinvasion. J. Virol. **80:**9361–9370.
24. **Runkler, N., E. Dietzel, M. Carsillo, S. Niewiesk, and A. Maisner.** 2009. Sorting signals in the measles virus wild-type glycoproteins differently influence virus spread in polarized epithelia and lymphocytes. J. Gen. Virol. **90:**2474–2482.
25. **Salditt, A., et al.** 2010. Measles virus M protein-driven particle production does not involve the endosomal sorting complex required for transport (ESCRT) system. J. Gen. Virol. **91:**1464–1472.
26. **Sänger, C., et al.** 2001. Sorting of Marburg virus surface protein and virus release take place at opposite surfaces of infected polarized epithelial cells. J. Virol. **75:**1274–1283.
27. **Tahara, M., et al.** 2008. Measles virus infects both polarized epithelial and immune cells by using distinctive receptor-binding sites on its hemagglutinin. J. Virol. **82:**4630–4637.
28. **Tahara, M., M. Takeda, and Y. Yanagi.** 2007. Altered interaction of the matrix protein with the cytoplasmic tail of hemagglutinin modulates measles virus growth by affecting virus assembly and cell-cell fusion. J. Virol. **81:**6827–6836.
29. **Takeda, M.** 2008. Measles virus breaks through epithelial cell barriers to achieve transmission. J. Clin. Invest. **118:**2386–2389.
30. **Tashiro, M., et al.** 1990. Altered budding site of a pantropic mutant of Sendai virus, F1-R, in polarized epithelial cells. J. Virol. **64:**4672–4677.
31. **Tatsuo, H., N. Ono, and Y. Yanagi.** 2001. Morbilliviruses use signaling lymphocyte activation molecules (CD150) as cellular receptors. J. Virol. **75:**5842–5850.
32. **Tseng, C. T., et al.** 2005. Apical entry and release of severe acute respiratory syndrome-associated coronavirus in polarized Calu-3 lung epithelial cells. J. Virol. **79:**9470–9479.
33. **von Messling, V., and R. Cattaneo.** 2002. Amino-terminal precursor sequence modulates canine distemper virus fusion protein function. J. Virol. **76:**4172–4180.
34. **von Messling, V., D. Milosevic, and R. Cattaneo.** 2004. Tropism illuminated: lymphocyte-based pathways blazed by lethal morbillivirus through the host immune system. Proc. Natl. Acad. Sci. U. S. A. **101:**14216–14221.
35. **von Messling, V., D. Milosevic, P. Devaux, and R. Cattaneo.** 2004. Canine distemper virus and measles virus fusion glycoprotein trimers: partial membrane-proximal ectodomain cleavage enhances function. J. Virol. **78:**7894–7903.
36. **von Messling, V., C. Springfeld, P. Devaux, and R. Cattaneo.** 2003. A ferret model of canine distemper virus virulence and immunosuppression. J. Virol. **77:**12579–12591.
37. **von Messling, V., N. Svitek, and R. Cattaneo.** 2006. Receptor (SLAM [CD150]) recognition and the V protein sustain swift lymphocyte-based invasion of mucosal tissue and lymphatic organs by a morbillivirus. J. Virol. **80:**6084–6092.
38. **von Messling, V., G. Zimmer, G. Herrler, L. Haas, and R. Cattaneo.** 2001. The hemagglutinin of canine distemper virus determines tropism and cytopathogenicity. J. Virol. **75:**6418–6427.
39. **Weise, C., et al.** 2010. Tyrosine residues in the cytoplasmic domains affect sorting and fusion activity of the Nipah virus glycoproteins in polarized epithelial cells. J. Virol. **84:**7634–7641.
40. **Zimmer, G., K. P. Zimmer, I. Trotz, and G. Herrler.** 2002. Vesicular stomatitis virus glycoprotein does not determine the site of virus release in polarized epithelial cells. J. Virol. **76:**4103–4107.